Predicting the Quality of Spatial Learning via Virtual Global Landmarks

Jia Liu, Avinash Kumar Singh, *Member, IEEE*, and Chin-Teng Lin, *Fellow, IEEE*

***Abstract*— Analyzing the effects landmarks have on spatial learning is an active area of research in the study of human navigation processes and one that is key to understanding the links between human brain dynamics, landmark encoding, and spatial learning outcomes. This article presents a study on whether electroencephalography (EEG) signals related to virtual global landmarks combined with deep learning can be used to predict the accuracy and efficacy of spatial learning. Virtual global landmarks are silhouettes of actual landmarks projected into the navigator's vision via a heads-up display. They serve as a notable frame of reference in addition to the local landmarks we all typically use for route navigation. From a mobile virtual reality scenario involving 55 participants, the results of the study suggest that the EEG data associated with those who were exposed to global landmarks shows a visibly better capacity for predicting the quality of spatial learning levels than those who were not. As such, the EEG features associated with processing VGLs have a greater functional relation to the quality of spatial learning. This finding opens up a future direction of enquiry into landmark encoding and navigational ability. It may also provide a potential avenue for the early diagnosis of Alzheimer's disease.**

***Index Terms*— Active navigation, electroencephalography (EEG), spatial learning, deep learning.**

I. Introduction

IN THE navigation process, spatial learning refers to the stages through which humans encode information about their environment as they navigate a route. It particularly refers to how we locate and recall relevant stimuli to prompt our next steps [1], [2]. This learning associated with spatial information processing involves several brain regions [3], [4], [5]. For example, our retrosplenial complex translates spatial representations with egocentric and allocentric reference frames [6]. Our head direction cells compute our orientation by translating spatial information with distinctive spatial references [7]. This involves the parahippocampal [8], entorhinal [9], and thalamus [10] regions of the brain, among others. Indeed, spatial learning can even physically affect the growth of brain structures. A well-known study on the enlarged hippocampi of London cab drivers by scientists at University College in London found that grey matter in the brains of taxi drivers grew and adapted to help them store detailed mental maps of the city [11]. In other words, through the process of continuously learning and processing their surroundings, the cab drivers' brains expanded to accommodate the cognitive demands of navigating London's streets.

Landmarks are one of the most crucial stimulants of cognitive navigation in spatial learning [12], [13]. Further, different kinds of landmarks are used in different ways [14]. Distant landmarks such as city skylines or mountain peaks serve as "global" landmarks. These are visible from far away and do not change much as the observer moves a small distance. As such, they act as a global frame of reference in the same way as a compass. By contrast, "local" landmarks are only visible from a small distance. We typically rely on these to achieve our intermediate navigation goals, such as 'turn right at the cinema' or 'drive straight through the roundabout with the statue'. These are therefore linked to route navigation. Accordingly, Bruns and Chamberlain find that, as easily remembered and recognisable spatial references, the configurations of landmark objects can assist in route learning and scene recognition [15].

However, with urbanisation, many global landmarks are obscured by skyscrapers and other buildings, especially as one approaches a CBD. It has been our contention for some time that this is having a deleterious effect on spatial navigation, and, to this end, we developed a heads-up display that reintroduces these global landmarks into our vision in the form of a virtual silhouette. As shown in Fig. 1a, called virtual global landmark (VGL), the system ensures that a global landmark can always be seen, even when a building or other aspect of the environment is blocking its view, by portraying a silhouette in its place. Fig. 1b presents a virtual reality point-of-view for our proposed VGL system. In a previous study, we show that reintroducing these landmarks does, in fact, improve spatial learning [16]. In this study we are concerned with whether EEG and other brain signals associated with VGLs can predict the quality of spatial learning.

Manuscript received 9 February 2022; revised 27 July 2022; accepted 13 August 2022. Date of publication 18 August 2022; date of current version 1 September 2022. This work was supported in part by the Australian Research Council (ARC) under Discovery Grant DP210101093 and Grant DP220100803, in part by the Australia Defence Innovation Hub under Contract P18-650825, in part by the Australian Cooperative Research Centres Projects (CRC-P) Round 11 under Grant CRCPXI000007, in part by the U.S. Office of Naval Research Global under Cooperative Agreement ONRG-NICOP-N62909-19-1-2058, in part by the Air Force Asian Office of Aerospace Research and Development (AOARD) and Defence Science and Technology (DST)–Australian Autonomy Initiative Agreement under Grant ID10134, and in part by the New South Wales (NSW) Defence Innovation Network and NSW State Government of Australia under Grant DINPP2019 S1-03/09 and Grant PP21-22.03.02. *(Corresponding author: Chin-Teng Lin.)*

This work involved human subjects or animals in its research. Approval of all ethical and experimental procedures and protocols was granted by the Research Ethics Committee (HREC) of University of Technology Sydney (UTS) under UTS HREC REF NO. ETH17-2095.

The authors are with CIBCI Center, Faculty of Engineering and Information Technology, School of Computer Science, Australian AI Institute, University of Technology Sydney, Sydney, NSW 2007, Australia (e-mail: jia.liu@uts.edu.au; avinash.singh@uts.edu.au; chin-teng.lin@uts.edu.au).

Digital Object Identifier 10.1109/TNSRE.2022.3199713

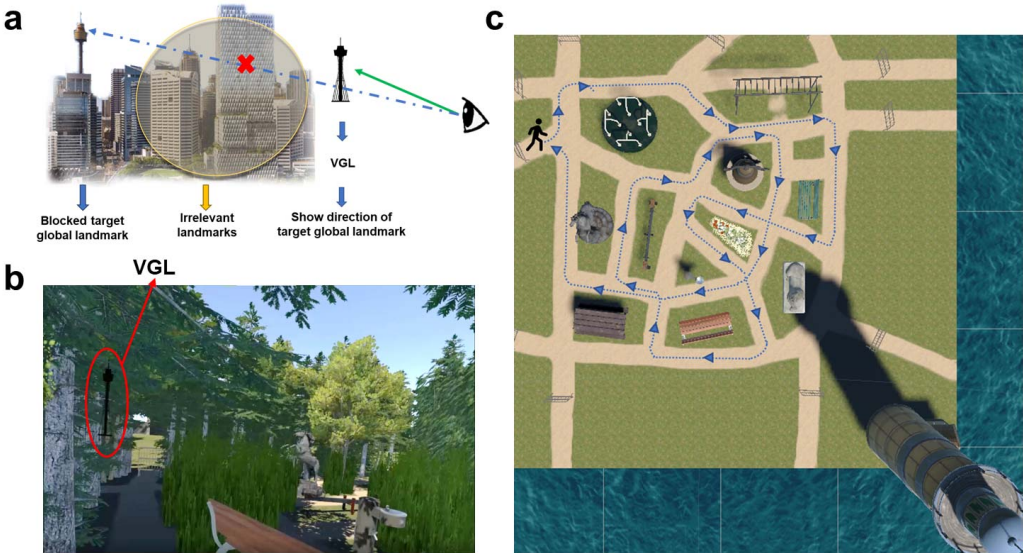

Fig. 1. VGL design and exploration map. (a) The working mechanism of the VGL. If the selected global landmark selected for inclusion in the scenario was blocked by environmental features, the VGL still indicated the direction of the global landmark in silhouette. (b) The first-person point-of-view during active navigation in the fully virtual environment. Again, the global landmark was always present, even when obscured from view by other objects. (c) One of the pre-defined exploration routes. Auditory instructions were used to guide participants through the route. In this illustration, the plants and trees inside and surrounding the scenario have been removed for a clearer view of the path.

Past research has linked theta oscillations to spatial navigation process in humans [17], and to the encoding and retrieval of spatial information in rodents [18]. Researchers have taken subdural recordings from epileptic patients while they navigate virtual mazes in a scenario displayed on a computer screen, and multiple episodes of high-amplitude theta activity were found in a number of areas including the frontal and temporal cortexes [19]. They further found that the frequency of theta-wave episodes occurred more frequently in complex mazes, which occurred more frequently in recall trials than in learning trials. In addition, as a critical visual stimulus in the environment, the importance of landmarks to spatial navigation has also been proven in past electrophysiological and imaging studies [20], [21], [22]. In an EEG study on landmark recognition tasks [23], frontal electrophysiological activity in the low frequency bands could reliably distinguish a targeted landmark from a non-targeted one. Here, frontal-theta oscillatory power was significantly lower for the target landmark. Another analysis on the late positive complex showed that the amplitude of the posterior late positive complex increases with an increasing amount of spatial information that is recollected from landmarks [24]. Assumed to be reflective of information recollection [25], increased late positive complex amplitudes were found for landmark information, with the most pronounced amplitudes recorded while the subjects were exploring and learning an environment with landmarks.

Inspired by the constructive role landmarks can play in spatial learning, we decided to test the predictive capacity of landmark-related EEG signals with multiple standard deep learning models, including EEGNet [26], DeepConvNet [27] and ShallowConvNet [27]. EEGNet is a compact Convolutional Neural Network (CNN) architecture utilizing the depthwise separable convolutions [28]. As a generalized model for EEG signals, it has shown optimal performance from a variety of paradigms with EEG signals [26]. DeepConvNet is also a broadly used convolution neural network model for EEG signals, which is able to learn different kinds of information in decoding tasks relating to EEG signals [27]. Inspired by filter bank common spatial patterns [29], ShallowConvNet is a shallow version of DeepConvCNN, with a larger kernel, a different activation function, a different pooling approach, and a classification block [27].

We enlisted 55 students from the University of Technology Sydney to participate in the study. To catch the EEG signals related to landmark stimuli during navigation activity in a more natural experimental environment [30], [31], [32], [33], [34], we applied the fully immersive virtual reality (VR) protocols to build our experiment scenario called "Sydney Park". The immersive VR technology allows users to act in real-time at artificial locations interacting synchronously via an interface that can track and display the users' actions [17], [35], [31]. In our study, through tracking the real-time reactions and motions of the participants with VR, we could be able to create a virtual environment where participants could actively and naturally explore and sense the pervasive computing environment with the stimulation of visual, auditory, and proprioceptive modalities in combination with high-density EEG [31], [36], [37]. During experiment, the participants were first divided into two groups and asked to explore "Sydney Park" by following auditory instructions along a predefined route as shown in Fig. 1c. Of the two groups, one group explored with the assistance of VGLs while the other explored without them. The route for exploration was predefined in a way that balanced the participant's exposure to local and global landmarks. During exploration, each participant was equipped with a head-mounted VR system and a mobile

TABLE I
PARTICIPANT DEMOGRAPHICS

Group	Women/Men	Age (years) [a]
VGL	15/13	27.57(±4.78)
non-VGL	9/18	28.19(±5.33)

[a] Standard deviations are shown in parentheses.

brain/body imaging (MoBI) [38], [39], [40] setup that captured brain dynamics via EEG signals while they explored.

Once they had completed the route, the participants were asked to draw a sketch map of the path they had just navigated. This was how we assessed the quality of spatial learning. To show incidental learning performance achieved both with and without VGLs in the environment, the participants were not informed that they would subsequently be asked to draw a map of the route they had taken during their explorations. We measured the fit of each sketch map to the actual route against seven-points of fidelity to score the outcome of spatial knowledge acquisition. Based on our design of VGL as a frame of reference for one's surroundings, we hypothesized that EEG signals of VGLs would achieve a higher efficacy in prediction performance than the other landmark stimuli.

II. MATERIALS AND METHODS

A. Participants

The experiment involved 55 participants – 24 females and 31 males (see Table I for demographic information) – and were conducted in the UTS Tech Lab. The experimental procedure was explained to each subject before participating in the study, with all providing informed consent. The Human Research Ethics Committee (HREC) of University of Technology Sydney (UTS) also reviewed the protocols and issued their approval (grant number: UTS HREC REF NO. ETH17-2095). All experiments were performed in accordance with relevant guidelines and regulations. None of the participants reported a history of any psychological disorders that could have affected the results.

B. Experiment Setup and Procedure

1) VGL System Setup: The virtual global landmarks were displayed as transparent, 2-dimensional silhouettes of the real landmark in the VR scenario, which served as a stable reference of the direction of specific locations without disturbing the overall environment. The silhouettes were presented in the direction of the global landmark within the participant's sightline. Whether walking or turning, as long as the participant looked in that direction, they were able to see either the real landmark or the silhouette if it was blocked by another object, as shown in Figure 1a. A total of three virtual global landmarks were included in our scenario: a lighthouse, the Sydney Opera House and the Sydney Tower Eye.

2) VR Scenario Setup: We developed a VR environment scenario called Sydney Park to imitate the real environment of the Sydney Botanical Gardens. Figure 1b shows the user's view of Sydney Park. Sydney Park was created in Unity 2018.3.5f1 (Unity Technologies, USA). The Sydney Park environment consists of 11 local landmarks and the 3 global landmarks in combination with paths, intersections, bushes, trees, etc. Two sides of the scenario were extended with only the sea, and a lighthouse standing in the corner next to the ocean. Of the remaining two sides, one had a view of the Sydney Opera House and the other had a view of the Sydney Tower Eye – similar to the actual views from the Royal Botanical Gardens. The scenario was fully immersive so as to hold participants' attention for the full duration of the navigation experiments. We used HTC's Vive Pro eye headset with an embedded Tobii eye tracker. The Vive Pro eye uses a dual OLED 3.5" diagonal display with a resolution of 1440 × 1600 pixels per eye (2880 × 1600 pixels combined) and a refresh rate of 90Hz, as reported by HTC. The participant's head position was principally tracked with embedded inertial measurement units, while an external lighthouse tracking system cleared the common tracking drift with a 60Hz update rate. Additionally, the eye activity of participants was tracked using the Tobii eye tracker at a sampling rate of 120Hz.

3) Experiment Procedure:

a) Exploration phase: All participants were randomly divided into two groups in this phase – one group that explored Sydney Park with the VGL system, and a non-VGL group, who explored without. Each participant in both groups first had five minutes to walk around inside a meadow area in the VR environment. Next, they started walking through the Sydney Park scenario along a fixed, predefined route with the assistance of auditory instructions (see Figure 1c). This was intended to help standardize how participants explored the environment. All local landmarks were passed twice while navigating the fixed route. The VGL group could always see a global landmark as they walked whether virtual or in silhouette; the non-VGL group could only see global landmarks if they were unobscured.

b) Map drawing task: After exploration, each participant was given a blank 11.7 × 16.5-inch sheet of paper, a pencil and an eraser. They were then instructed to draw any information they remembered about the scenario, including landmarks, paths, and so on. They were not allowed to listen to the instructions again or redo the scenario.

C. EEG Recording and Pre-Processing

The EEG data were recorded continuously using Brain Vision's LiveAmp 64 system (Brain Products, Gilching, Germany) with 64 active electrodes mounted on an elastic cap. The sampling rate was 500 Hz with a low-pass filter of 131Hz. The electrodes were positioned according to an extended 10-20 system [41]. The EEG signals were referenced to the electrode located at FCz and the impedance of all sensors was kept below 5kΩ. EEG events were created when the participants' fixated on the surface of a defined landmark, both virtual and in silhouette. All data streams from the EEG cap, eye tracker and head-mounted display were synchronized with Lab Streaming Layer (LSL).

Raw EEG data were imported into MATLAB version 2018a (MathWorks Inc., USA) for processing. We used EEGLAB toolbox version 2020.0 [42] to aid with the analysis. For each participant's raw data, we first checked the data quality by eye

to ensure the EEG data was consistently recording with active movements during experiment. Of the 55 participants, data of one participant from non-VGL group was excluded due to poor EEG quality. The raw data for the remaining 54 participants were first bandpass filtered from 1Hz to 100Hz and downsampled to 250Hz. Then, data from each single task were merged into one large EEG dataset for the following pre-processing steps. Line noise and flatlines were removed in turn using the *cleanline* and *clean_flatlines* functions in EEGLAB, and noisy channels were rejected with the *clean_channels* function. All missing EEG channels were interpolated by spherical splines before re-referencing to the average of all channels. Noisy data in the time domain were removed through automatic continuous data cleaning. The data were then submitted to adaptive mixed independent component analysis to obtain independent components [42], [43]. The equivalent dipole model of each independent component was computed using a boundary element head model as implemented in EEGLAB's DIFIT2 routines [44]. Last, the sphere and weights of the ICA and dipole models were copied back to the pre-processed but uncleaned EEG single-task data for further analysis. (There was no cleaning in the time domain.)

D. Sample, Sampling Strategy

1) Classification of Spatial Learning Level: $N = 28$ sketch maps from the VGL group's participants and $N = 27$ sketch maps from non-VGL group were assessed with the Gardony Map Drawing Analyzer (GMDA) [45]. We used the map score as an indicator to show the spatial learning outcome for each participant. Based on the scores, participants were separated into two levels of the spatial learning outcome, high and low levels. To improve the reliability of two levels, we dropped 20% of the participants' scores around the median score. The dropped data was set as discarded data and removed from the dataset. We then set the top 40% of scores as the high level for spatial learning and the bottom 40% of scores as the low level.

2) Extraction of Time-Dependency Features on EEG Data: Based on the selected data for two behaviour levels above, the corresponding EEG datasets were further processed for feature extraction. To get the segments of EEG data related to landmark stimuli during exploration, the pre-processed data were extracted in time windows of -1 to 7 seconds. For each segment, only one kind of landmark was in view (the virtual global landmarks in the VGL group or the local landmarks in the non-VGL group).

III. Results and Discussion

A. Spatial Learning Outcomes

Sketching maps is a common method of evaluating spatial knowledge learned from an environment [45], [46], [47]. Thus, in our study, we took the sketch map scores as reflective of spatial learning outcomes for each participant. Table II lists the map scores and the corresponding classified level camps for all participants. The participants are ranked based on their scores from bottom to top. 20% of the participants were discarded as the gap between the low level and high-level camps for each group. For the remaining participants, the top 40% were sorted into the high-level camp and the bottom 40% were assigned to the low-level camp.

TABLE II
CLASSIFICATION OF SPATIAL LEARNING LEVEL AND MAP SCORES

level	VGL group participant ID	VGL group map score	non-VGL group participant ID	non-VGL group map score
low	11	2.4378	10	1.6326
	17	2.4797	54	2.4911
	5	2.4821	30	2.5700
	13	2.5275	20	2.7050
	7	2.8093	8	2.8105
	35	2.8840	18	2.8114
	3	3.0256	14	2.8276
	55	3.0438	40	2.8583
	19	3.1448	2	2.9010
	29	3.1484	12	2.9333
	39	3.1584		
gap	9	3.2266	16	2.9637
	45	3.2290	36	2.9727
	25	3.2464	4	2.9812
	15	3.2485	26	3.0306
	23	3.2794	38	3.0362
	1	3.2844	48	3.0653
high	27	3.2907	22	3.1164
	21	3.3302	28	3.1786
	37	3.3750	34	3.1839
	33	3.4781	52	3.2272
	41	3.5292	50	3.3201
	43	3.5727	24	3.3325
	31	3.6296	32	3.3776
	47	3.6410	6	3.4206
	49	3.7344	42	3.4295
	51	3.7474	44	3.5286
	53	3.7725	46	3.5852

B. Prediction of Spatial Learning Level Using EEG Data

Our objective was to test whether the EEG signals at the stage of exploration could reliably predict the quality of spatial learning outcomes given the two types of landmark stimuli. As such, we compared the EEG inputs versus map quality for the VGL and non-VGL groups. Three popular deep learning algorithms were applied as the training models: EEGNet [26], DeepConvNet [27] and ShallowConvNet [27]. EEG signals associated with those in the low-level camp were labelled 0 and those in the high-level camp were labelled 1. The accuracy performance of prediction was measured in terms of three metrics – accuracy (*Acc*), F1 score and Cohen's kappa coefficient, calculated as:

$$Acc = (T(0) + T(1))/N \tag{1}$$

$$F1\ score = (2 \cdot T(0))/(2 \cdot T(0) + F(0) + F(1)) \tag{2}$$

$$\begin{aligned} Kappa\ coefficient = {} & 2 \cdot (T(0) \cdot T(1) - F(0) \cdot F(1)) \\ & /((T(0) + F(0)) \cdot (F(0) + T(1)) \\ & \cdot (T(0) + F(1)) \cdot (F(1) + T(1))) \end{aligned} \tag{3}$$

TABLE III
EEG DATA CONFIGURATION AND PREDICTION PERFORMANCE

	VGL group			non-VGL group		
Input data points	64×2000×773			64×2000×829		
model	*Acc*	F1 score	Kappa coefficient	*Acc*	F1 score	Kappa coefficient
EEGnet	0.7032	0.7051	0.4073	0.6627	0.6782	0.3300
DeepConvNet	0.8516	0.8571	0.7028	0.7952	0.7927	0.5908
ShallowConvNet	0.7484	0.7516	0.4972	0.6807	0.6443	0.3566

TABLE IV
10-FOLD CROSS-VALIDATION RESULTS

model	VGL group		non-VGL group	
	Acc	F1 score	*Acc*	F1 score
EEGnet	1.0000	1.0000	0.5000	0.6667
DeepConvNet	0.8701	0.9306	0.6829	0.8116
ShallowConvNet	1.0000	1.0000	0.9756	0.9877

where T(0) is the number of true results classified by model as label 0 (low level), T(1) is the number of true results classified by model as label 1 (high level), F(0) is the number of false results classified by model as label 0 (low level), F(1) is the number of false results classified by model as label 1 (high level) and N is the total number of data samples.

Besides the *Acc*, F1 score and Cohen's kappa coefficient are commonly used as evaluation metrics for binary classification. Assuming the positive and negative as the two classes, the F1 score is balancing precision and recall on the positive class while accuracy looks at correctly classified observations both positive and negative. The kappa statistic compares the accuracy of the classification system to the accuracy of a random classification system [48], [49]. In other words, the kappa coefficient measures how closely the instances classified by the classifier matched the data labelled as ground truth, controlling for the accuracy of a random classifier as measured by the expected accuracy. Thus, the kappa statistic not only reflects how the classifier itself performed, also compares any other model used for the same classification task.

Table III shows the input data configurations and prediction performance from three models. We ran a maximum of 1000 training epochs with a batch size of 8. The number of data points equalled the number of channels × the sampling rate × the number of EEG epochs analysed. The results clearly show that predicting spatial learning levels based on the brain signal data from the VGL group produced a significantly more accurate result than the non-VGL group. Averaging the results from the three models, the VGL group outperformed the non-VGL group by 7.72% in terms of *Acc*, 9.57% in terms of F1 score, and 27.37% in terms of Cohen's kappa coefficient.

To further estimate the training performance, we performed 10-fold cross-validation with the same input data and classifier models. The results are shown in Table IV. Similar to the results in Table III, the cross-validation results also indicated an average 43.30% improvement in *Acc* and 21.97% improvement in F1 scores with EEG data associated with VGL stimuli from the VGL group compared to local landmarks from the non-VGL group.

In the time-dependency points, the EEG data collected from the VGL group shows a visibly better capacity for predicting the quality of spatial learning levels compared to the data collected from the non-VGL group. In other words, the EEG features associated with VGLs relate better to functional spatial learning than local landmarks do. This might be because, as a conspicuous and easy-to-pinpoint reference, global landmarks can help participants build a clearer directional relationship between themselves and a constant point of reference than local landmarks [50], [51]. Thus, as a persistent reference to a global landmark, VGLs help participants to mark routes well and to accurately learn the features of their environment. By the same token, the EEG features associated with VGLs processed during the spatial learning stages of exploration would appear to more directly reflect the quality of the spatial learning outcomes.

C. Visualizing the EEG Dataset

To uncover the feature differences on EEG data between VGL group and non-VGL group, we plotted the event-related spectral perturbations (ERSPs) with the *newtimef* function in EEGLAB [42]. In addition to the features from the time-domain, ERSPs also show frequency spectrum dynamics. We evaluated the ERSPs originating in the frontal and parietal cortices of participants. Many studies have demonstrated involvement by the parietal cortex in spatial navigation [52], [53], [54], [55]. Further, as the behaviour and emotional control centre of our brains, the frontal lobes are important for voluntary movement and for managing higher-level executive functions [56]. Especially, based on our previous studies [57], [58], the frontal and parietal areas are found to be associated to the quality of spatial learning caused by the stimulus of VGLs and local landmarks. These two areas are also revealed by studies for their roles to reflect the spatial attention and navigation strategies [59], [60], [18]. Thus, we were interested to see whether brain dynamics in the parietal and frontal cortical areas would differ when VGLs were in view as used by the VGL group versus the local landmarks of the non-VGL group in this study. Based on the classifications in Table II,

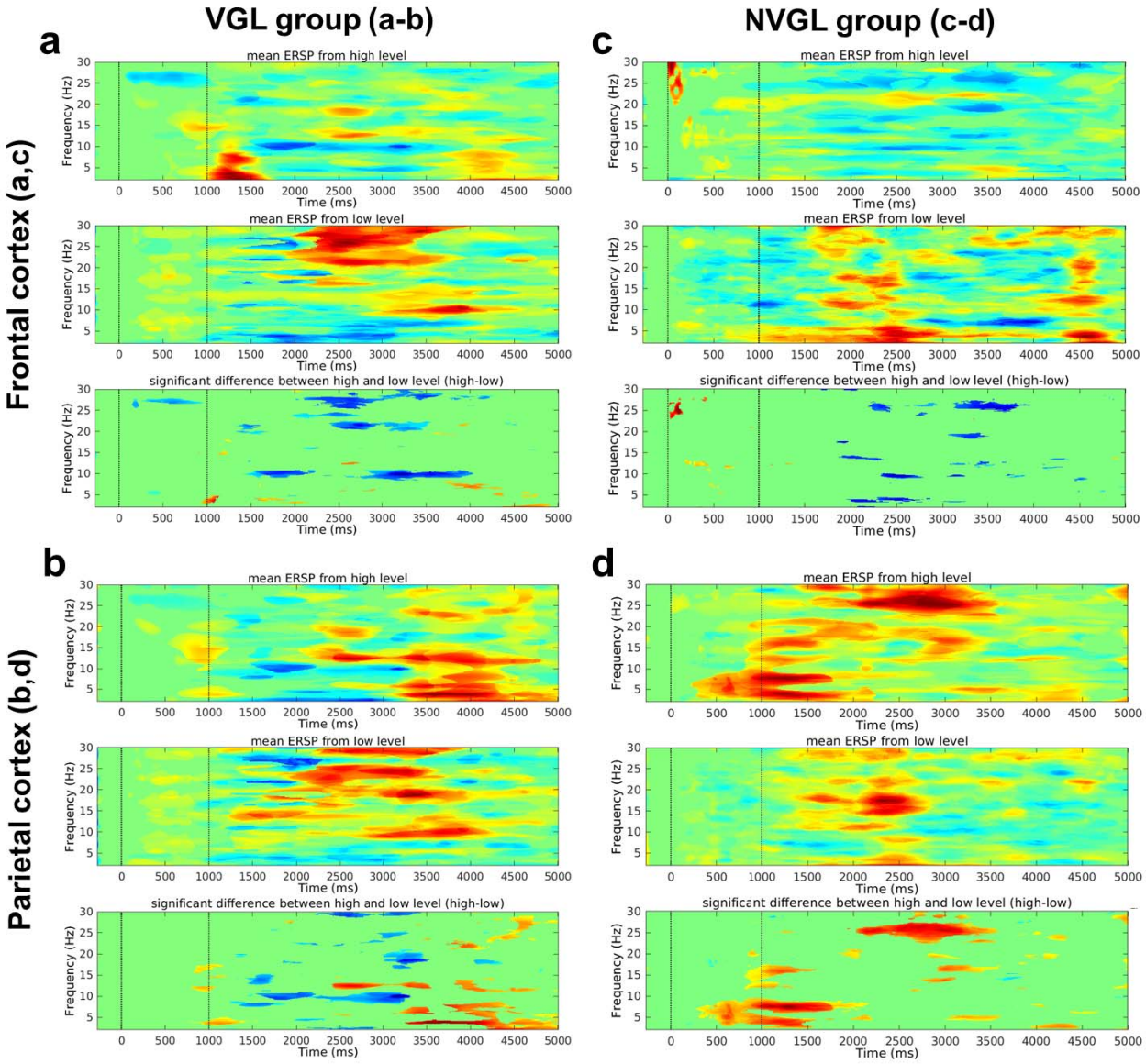

Fig. 2. Mean ERSPs for low and high levels from VGL and non-VGL groups. (a-b) mean ERSPs in VGL group for high and low levels and significant differences between two levels (ERSPs of high level minus the ERSPs of low level) with $p < .05$ from frontal (a) and parietal (b) cortex. (c-d) mean ERSPs in non-VGL group for high and low levels and significant differences between two levels (ERSPs of high level minus the ERSPs of low level) with $p < .05$ from frontal (c) and parietal (d) cortex. For all ERSPs, first dotted lines at the 0 ms time point signify the onset of a trial, and the second dotted lines at the 1000 ms time point signify the onset of stimuli (The stimulus in VGL group is virtual global landmark, and in non-VGL group is local landmark). The non-significant points were masked with zero values in the mean ERSPs and are displayed in green. Significant differences with respect to baseline activity are displayed in red and blue for positive and negative deviations from the baseline activity, respectively.

the mean ERSPs for low and high levels from both groups were plotted separately.

The results are presented in Figure 2. In the VGL group (Figure 2a), significant differences in the frontal cortex between the average ERSPs for high and low levels revealed broad and significant decreases in alpha and beta activity that started a short time after the onset of VGL stimuli, $p < .05$. Similarly, significant differences between the two levels of frontal cortex with the local landmarks (Figure 2c) showed substantial suppression in the same frequency bands, $p < .05$. That said, the suppression began slightly later after the stimuli than for the VGL group. In Figure 2b, the significant differences of parietal cortex in VGL group between two levels demonstrated a broader and strong difference in the theta, alpha, and beta bands that covered nearly all-time domains. In the same brain area with the non-VGL group, the differences in ERSPs between the two levels (Figure 2d) were statistically significant for the delta and beta bands over a narrower time periods.

As a visualization of our EEG signals from two groups, the ESRP results suggest significant differences between the two levels of spatial learning outcomes. Compared to the non-VGL group, the brain dynamics associated with the VGL group showed broader mean spectral power changes in the time

domain. This might be the reason why the EEG data related to VGLs were more accurate predictors of spatial learning outcomes with time-dependency features than that of the local landmarks.

IV. Conclusion

The results of this study indicate that it could be possible to use deep learning to predict the quality of spatial learning outcomes by analyzing EEG signals relating to the encoding of virtual global landmarks in the human brain. As a reliable and steady reference point for a global landmark, the VGL system shows an evident improvement in the predictive capacity of on spatial learning levels compared to the signal associated with encoding local landmarks. By visualizing the brain dynamics associated with landmark stimuli, the broader mean spectral power changes in time domain were found in VGL group dataset. This finding has the potential to unlock key insights into the workings of spatial ability prediction. For example, it may be possible that this link opens a door to aid the early diagnosis of conditions such as Alzheimer's disease by quantifying impairments in brain dynamics on landmark stimuli.

References

[1] B. Barak, N. Feldman, and E. Okun, "Cardiovascular fitness and cognitive spatial learning in rodents and in humans," *J. Gerontol. A, Biol. Sci. Med. Sci.*, vol. 70, no. 9, pp. 1059–1066, Sep. 2015.

[2] F. Chersi and N. Burgess, "The cognitive architecture of spatial navigation: Hippocampal and striatal contributions," *Neuron*, vol. 88, no. 1, pp. 64–77, Oct. 2015.

[3] A. D. Ekstrom *et al.*, "Cellular networks underlying human spatial navigation," *Nature*, vol. 425, no. 6954, pp. 184–188, Sep. 2003.

[4] C. F. Doeller, C. Barry, and N. Burgess, "Evidence for grid cells in a human memory network," *Nature*, vol. 463, no. 7281, pp. 657–661, 2010.

[5] J. O'Keefe and L. Nadel, *The Hippocampus as a Cognitive Map*. Oxford, U.K.: Clarendon Press, 1978.

[6] S. D. Vann, J. P. Aggleton, and E. A. Maguire, "What does the retrosplenial cortex do?" *Nature Rev. Neurosci.*, vol. 10, no. 11, pp. 792–802, Nov. 2009.

[7] B. J. Clark, J. P. Bassett, S. S. Wang, and J. S. Taube, "Impaired head direction cell representation in the anterodorsal thalamus after lesions of the retrosplenial cortex," *J. Neurosci.*, vol. 30, no. 15, pp. 5289–5302, Apr. 2010.

[8] L. K. Vass and R. A. Epstein, "Common neural representations for visually guided reorientation and spatial imagery," *Cerebral Cortex*, vol. 27, no. 2, pp. 1457–1471, 2017.

[9] M. J. Chadwick, A. E. J. Jolly, D. P. Amos, D. Hassabis, and H. J. Spiers, "A goal direction signal in the human entorhinal/subicular region," *Current Biol.*, vol. 25, no. 1, pp. 87–92, Jan. 2015.

[10] J. P. Shine, J. P. Valdés-Herrera, M. Hegarty, and T. Wolbers, "The human retrosplenial cortex and thalamus code head direction in a global reference frame," *J. Neurosci.*, vol. 36, no. 24, pp. 6371–6381, Jun. 2016.

[11] E. A. Maguire *et al.*, "Navigation-related structural change in the hippocampi of taxi drivers," *Proc. Nat. Acad. Sci. USA*, vol. 97, no. 8, pp. 4398–4403, Apr. 2000.

[12] E. Chan, O. Baumann, M. A. Bellgrove, and J. B. Mattingley, "From objects to landmarks: The function of visual location information in spatial navigation," *Frontiers Psychol.*, vol. 3, p. 304, 2012.

[13] R. M. Yoder, B. J. Clark, and J. S. Taube, "Origins of landmark encoding in the brain," *Trends Neurosciences*, vol. 34, no. 11, pp. 561–571, Nov. 2011.

[14] A. Schwering, R. Li, and V. Anacta, "The use of local and global landmarks across scales and modes of transportation in verbal route instructions," presented at the Spatial Cognition Conf., Bremen, Germany, Sep. 2014.

[15] C. R. Bruns and B. C. Chamberlain, "The influence of landmarks and urban form on cognitive maps using virtual reality," *Landscape Urban Planning*, vol. 189, pp. 296–306, Sep. 2019.

[16] A. K. Singh, J. Liu, C. A. Tirado Cortes, and C.-T. Lin, "Virtual global landmark: An augmented reality technique to improve spatial navigation learning," in *Proc. Extended Abstr. CHI Conf. Hum. Factors Comput. Syst.*, Yokohama, Japan, May 2021, pp. 1–6.

[17] C.-S. Yang, J. Liu, A. K. Singh, K.-C. Huang, and C.-T. Lin, "Brain dynamics of spatial reference frame proclivity in active navigation," *IEEE Trans. Neural Syst. Rehabil. Eng.*, vol. 29, pp. 1701–1710, 2021.

[18] K. Gramann, H. J. Müller, B. Schönebeck, and G. Debus, "The neural basis of ego- and allocentric reference frames in spatial navigation: Evidence from spatio-temporal coupled current density reconstruction," *Brain Res.*, vol. 1118, no. 1, pp. 116–129, Nov. 2006.

[19] M. J. Kahana, R. Sekuler, J. B. Caplan, M. Kirschen, and J. R. Madsen, "Human theta oscillations exhibit task dependence during virtual maze navigation," *Nature*, vol. 399, no. 6738, pp. 781–784, Jun. 1999.

[20] P. Jansen-Osmann and G. Wiedenbauer, "The representation of landmarks and routes in children and adults: A study in a virtual environment," *J. Environ. Psychol.*, vol. 24, no. 3, pp. 347–357, Sep. 2004.

[21] G. Janzen and C. Jansen, "A neural wayfinding mechanism adjusts for ambiguous landmark information," *NeuroImage*, vol. 52, no. 1, pp. 364–370, Aug. 2010.

[22] J. Wegman, A. Tyborowska, and G. Janzen, "Encoding and retrieval of landmark-related spatial cues during navigation: An fMRI study," *Hippocampus*, vol. 24, no. 7, pp. 853–868, 2014.

[23] C. T. Weidemann, M. V. Mollison, and M. J. Kahana, "Electrophysiological correlates of high-level perception during spatial navigation," *Psychonomic Bull. Rev.*, vol. 16, no. 2, pp. 313–319, Apr. 2009.

[24] E. A. Edelstein *et al.*, "Neural responses during navigation in the virtual aided design laboratory: Brain dynamics of orientation in architecturally ambiguous space," *Movement Orientation Built Environ., Evaluating Des. Rationale Cognition*, vol. 35, pp. 35–41, May 2008.

[25] A. P. Yonelinas, "The nature of recollection and familiarity: A review of 30 years of research," *J. Memory Lang.*, vol. 46, no. 3, pp. 441–517, Apr. 2002.

[26] V. J. Lawhern, A. J. Solon, N. R. Waytowich, S. M. Gordon, C. P. Hung, and B. J. Lance, "EEGNet: A compact convolutional neural network for EEG-based brain–computer interfaces," *J. Neural Eng.*, vol. 15, no. 5, Jul. 2018, Art. no. 056013.

[27] R. T. Schirrmeister *et al.*, "Deep learning with convolutional neural networks for EEG decoding and visualization," *Hum. Brain Mapping*, vol. 38, no. 11, pp. 5391–5420, 2017.

[28] F. Chollet, "Xception: Deep learning with depthwise separable convolutions," in *Proc. IEEE Conf. Comput. Vis. Pattern Recognit. (CVPR)*, Jul. 2017, pp. 1800–1807.

[29] K. Keng Ang, Z. Yang Chin, H. Zhang, and C. Guan, "Filter bank common spatial pattern (FBCSP) in brain-computer interface," in *Proc. IEEE Int. Joint Conf. Neural Netw. (IEEE World Congr. Comput. Intell.)*, Jun. 2008, pp. 2390–2397.

[30] M. Plank, J. Snider, E. Kaestner, E. Halgren, and H. Poizner, "Neurocognitive stages of spatial cognitive mapping measured during free exploration of a large-scale virtual environment," *J. Neurophysiol.*, vol. 113, no. 3, pp. 740–753, Feb. 2015.

[31] A. Delaux *et al.*, "Mobile brain/body imaging of landmark-based navigation with high-density EEG," *Eur. J. Neurosci.*, vol. 54, no. 12, pp. 8256–8282, 2021.

[32] J. Snider, M. Plank, G. Lynch, E. Halgren, and H. Poizner, "Human cortical θ during free exploration encodes space and predicts subsequent memory," *J. Neurosci.*, vol. 33, no. 38, pp. 15056–15068, 2013.

[33] M. Plank, H. J. Müller, J. Onton, S. Makeig, and K. Gramann, "Human EEG correlates of spatial navigation within egocentric and allocentric reference frames," in *Proc. Int. Conf. Spatial Cognition*, 2010, pp. 191–206.

[34] L. Gehrke, J. R. Iversen, S. Makeig, and K. Gramann, "The invisible maze task (IMT): Interactive exploration of sparse virtual environments to investigate action-driven formation of spatial representations," in *Proc. German Conf. Spatial Cognition*, 2018, pp. 293–310.

[35] A. Innocenti, "Virtual reality experiments in economics," *J. Behav. Exp. Econ.*, vol. 69, pp. 71–77, Aug. 2017.

[36] C. J. Bohil, B. Alicea, and F. A. Biocca, "Virtual reality in neuroscience research and therapy," *Nature Rev. Neurosci.*, vol. 12, no. 12, pp. 752–762, Dec. 2011.

[37] S. E. Kober, J. Kurzmann, and C. Neuper, "Cortical correlate of spatial presence in 2D and 3D interactive virtual reality: An EEG study," *Int. J. Psychophysiol.*, vol. 83, no. 3, pp. 365–374, Mar. 2012.

[38] S. Makeig, K. Gramann, T.-P. Jung, T. J. Sejnowski, and H. Poizner, "Linking brain, mind and behavior," *Int. J. Psychophysiol.*, vol. 73, no. 2, pp. 95–100, Aug. 2009.

[39] K. Gramann *et al.*, "Cognition in action: Imaging brain/body dynamics in mobile humans," *Rev. Neurosci.*, vol. 22, no. 6, pp. 593–608, 2011.
[40] K. Gramann, T.-P. Jung, D. P. Ferris, C.-T. Lin, and S. Makeig, "Toward a new cognitive neuroscience: Modeling natural brain dynamics," *Frontiers Hum. Neurosci.*, vol. 8, p. 444, Jun. 2014.
[41] G. E. Chatrian, E. Lettich, and P. L. Nelson, "Ten percent electrode system for topographic studies of spontaneous and evoked EEG activities," *Amer. J. EEG Technol.*, vol. 25, no. 2, pp. 83–92, Jun. 1985.
[42] A. Delorme and S. Makeig, "EEGLAB: An open source toolbox for analysis of single-trial EEG dynamics including independent component analysis," *J. Neurosci. Methods*, vol. 134, no. 1, pp. 9–21, Mar. 2004.
[43] J. A. Palmer, K. Kreutz-Delgado, and S. Makeig, "Super-Gaussian mixture source model for ICA," in *Proc. Int. Conf. Independ. Compon. Anal. Signal Separat.*, 2006, pp. 854–861.
[44] R. Oostenveld and T. F. Oostendorp, "Validating the boundary element method for forward and inverse EEG computations in the presence of a hole in the skull," *Hum. Brain Mapping*, vol. 17, no. 3, pp. 179–192, Nov. 2002.
[45] A. L. Gardony, H. A. Taylor, and T. T. Brunyé, "Gardony map drawing analyzer: Software for quantitative analysis of sketch maps," *Behav. Res. Methods*, vol. 48, no. 1, pp. 151–177, Mar. 2016.
[46] J. Wang and A. Schwering, "Invariant spatial information in sketch maps—A study of survey sketch maps of urban areas," *J. Spatial Inf. Sci.*, vol. 31, no. 11, pp. 31–52, 2015.
[47] A. L. Gardony, T. T. Brunyé, and H. A. Taylor, "Navigational aids and spatial memory impairment: The role of divided attention," *Spatial Cognition Comput.*, vol. 15, no. 4, pp. 246–284, Oct. 2015.
[48] J. Cohen, "A coefficient of agreement for nominal scales," *Educ. Psychol. Meas.*, vol. 20, no. 1, pp. 37–46, Apr. 1960.
[49] M. L. McHugh, "Interrater reliability: The Kappa statistic," *Biochemia Medica*, vol. 22, no. 3, pp. 276–282, 2012.
[50] S. Steck and H. Mallot, "The role of global and local landmarks in virtual environment navigation," *Presence*, vol. 9, no. 1, pp. 69–83, Feb. 2000.
[51] S. Credé, T. Thrash, C. Hölscher, and S. I. Fabrikant, "The advantage of globally visible landmarks for spatial learning," *J. Environ. Psychol.*, vol. 67, Feb. 2020, Art. no. 101369.
[52] T. Oess, J. L. Krichmar, and F. Röhrbein, "A computational model for spatial navigation based on reference frames in the hippocampus, retrosplenial cortex, and posterior parietal cortex," *Frontiers Neurorobot.*, vol. 11, p. 4, Feb. 2017.
[53] J. R. Whitlock, R. J. Sutherland, M. P. Witter, M.-B. Moser, and E. I. Moser, "Navigating from hippocampus to parietal cortex," *Proc. Nat. Acad. Sci. USA*, vol. 105, no. 39, pp. 14755–14762, Sep. 2008.
[54] E. Rolls, "The parietal cortex, spatial functions, and navigation," in *Brain Computations*, Dec. 2020, pp. 363–378, doi: 10.1093/oso/9780198871101.003.0010.
[55] B. J. Clark, C. M. Simmons, L. E. Berkowitz, and A. A. Wilber, "The retrosplenial-parietal network and reference frame coordination for spatial navigation," *Behav. Neurosci.*, vol. 132, no. 5, pp. 416–429, 2018.
[56] H. S. Levin, H. M. Eisenberg, and A. L. Benton, *Frontal Lobe Function and Dysfunction*. New York, NY, USA: Oxford Univ. Press, 1991.
[57] J. Liu, A. K. Singh, A. Wunderlich, K. Gramann, and C.-T. Lin, "Redesigning navigational aids using virtual global landmarks to improve spatial knowledge retrieval," *npj Sci. Learn.*, vol. 7, no. 1, p. 17, Dec. 2022.
[58] J. Liu, A. K. Singh, and C.-T. Lin, "Using virtual global landmark to improve incidental spatial learning," *Sci. Rep.*, vol. 12, no. 1, p. 6744, Dec. 2022.
[59] M. Scolari, K. N. Seidl-Rathkopf, and S. Kastner, "Functions of the human frontoparietal attention network: Evidence from neuroimaging," *Current Opinion Behav. Sci.*, vol. 1, pp. 32–39, Feb. 2015.
[60] K. Gramann, J. Onton, D. Riccobon, H. J. Mueller, S. Bardins, and S. Makeig, "Human brain dynamics accompanying use of egocentric and allocentric reference frames during navigation," *J. Cognit. Neurosci.*, vol. 22, no. 12, pp. 2836–2849, Dec. 2010.